Pergamon

Int. J. Solids Structures Vol. 34, No. 23, pp. 2991–3019, 1997

0020–7683/97 $17.00 + .00

PII: S0020–7683(96)00207–7

FAILURE CRITERION FOR MOISTURE-SENSITIVE PLASTIC PACKAGES OF INTEGRATED CIRCUIT (IC) DEVICES: APPLICATION OF VON-KÁRMÁN'S EQUATIONS WITH CONSIDERATION OF THERMOELASTIC STRAINS

E. SUHIR
Lucent Technologies, Bell Laboratories, Physical Sciences and Engineering Division,
600 Mountain Ave., Room 7D-326, Murray Hill, NJ 07974-0636, U.S.A.

(*Received* 17 *November* 1995; *in revised form* 18 *September* 1996)

Abstract—The maximum value of the von-Mises stress in the molding compound at the chip corner is suggested to be used as a suitable failure criterion for moisture-induced plastic packages of integrated circuit (IC) devices. This criterion is able to reflect the role of various geometric and materials characteristics affecting the package propensity to moisture-induced failures during high-temperature reflow soldering. It is suggested also that the von-Mises stress be determined from the constitutive equations which are a generalization of the von-Kármán equations for large deflections of plates with consideration of thermoelastic strains. The generalized von-Kármán equations are applied to the underchip layer of the molding compound and consider thermal effects associated with the thermal expansion (contraction) mismatch of the materials in the package, as well as with temperature gradients. The predicted stresses are in good agreement with experimental observations.

The calculated von-Mises stresses can be used, particularly, for the development of "Figures of Merit" that would enable one to separate packages that need to be "baked" and "bagged" (or "rebaked" and "rebagged") from those that supposedly do not. The calculated stresses can be used also to judge whether the qualification test conditions for sufficiently reliable packages (say, thick packages with small chips) could be safely "derated" to an actual factory humidity profile. Finally, the calculated von-Mises stress can be helpful in the selection of the most feasible molding compound for the given package design. A more reliable (and more expensive) material might be needed in the case of a thin package with a large chip, while a low cost compound can be successfully employed in the case of a thick package with a small chip. © 1997 Elsevier Science Ltd.

INTRODUCTION

Recent improvements in the properties of molding compounds, plastic package designs, and manufacturing technologies have resulted in a substantial increase in the reliability of plastic packages. There is, however, one major industry-wide concern associated with these packages—moisture-induced failures. Such failures typically occur during surface-mounting the packages onto printed circuit boards (PCB) by means of high temperature reflow soldering and are usually attributed to, although might not be limited by, high internal water vapor pressure caused by a sudden evaporation of moisture, contained in the plastic material. In the extreme case, which is most likely to occur in a situation when the molding compound is completely delaminated from the chip or the paddle, rapid propagation of a crack, initiated at the chip's corner or at the paddle's edge, can be accompanied by a snapping sound and bulging of the package surface away from the delaminated area ("popcorn effect").

Although the phenomenon and various consequences of moisture-induced failures in plastic packages of IC devices is not yet completely understood, it has been established that the following factors and their unfavorable combinations play an important role, as far as such failures are concerned:

—*High moisture content* that not only leads to high water vapor pressure, but might result also in a substantial decrease in the ultimate, fatigue, and brittle strength of the molding compound.

—*Interfacial delaminations* that lead to elevated stress concentrations, high water vapor pressure (due to the moisture accumulated in the gap between the delaminated surfaces) and, most importantly, result in considerable weakening of the package because of its inability to perform as a composite structure: the delaminated portion of the molding compound above or below the chip (paddle) becomes isolated from the rest of the package and bends, independently of the package, as a plate.

—*Low fracture toughness of the molding compound* that makes the compound unable to effectively withstand the initiation and propagation of cracks.

—*Insufficient thickness* (*low section modulus*) of the molding compound above or below the chip (paddle), especially if delamination takes place.

—*Elevated thermally induced stresses* caused by thermal expansion (contraction) mismatch of the dissimilar materials in the package (mainly between the chi and the molding compound), as well as by the temperature gradients in the molding compound (especially in the through-thickness direction).

—*Initial stresses* and, perhaps, also *initial bowing* of the package resulting from the thermal expansion (contraction) mismatch of the materials in the package when it is cooled down from the manufacturing (curing) temperature to room temperature.

Clearly, each of these factors can be of greater or lesser significance, depending on the geometry, materials, and loading in a particular package design. It is clear also that the results of experimental investigations, valuable as they might be, inevitably reflect the combined effect of a variety of factors, whereas what is needed for the understanding of the mechanical behavior, life prediction, and structural and materials optimization, is the knowledge of the role of each particular parameter affecting the reliability of the package. Therefore, theoretical modeling can be very helpful for understanding, predicting, and optimizing the mechanical behavior of a plastic package during reflow soldering operation.

It has been shown (Fukuzawa *et al.*, 1985) that a uniformly loaded rectangular plate clamped around its support contour can be used as a theoretical model for the evaluation of the maximum stress in a plastic package undergoing surface mounting operation and subjected to water vapor loading (Fig. 1). In the analysis that follows a more comprehensive and a more flexible analytical stress model (Suhir, 1995), based on von-Kármán's equations of large deflection of plates (see, e.g., Timoshenko and Woinowski-Krieger, 1959), is developed for the assessment of the plastic package propensity to moisture-induced structural failures. This model considers the effect of the thermoelastic strains, and is based on an assumption that the maximum von-Mises stress can be effectively used as a suitable failure criterion that reflects the effect of various geometric and materials characteristics of the moisture sensitive plastic package on its propensity to a structural failure. It is envisioned that the application of such a criterion might be helpful in bringing different plastic package designs to a "common denominator", when comparing (rating) these designs from the standpoint of their propensity to failure. In this connection we would like to point out that von-Mises stress is a *structural criterion* and, as such, is different from both *geometric* criteria (such as, say, chip-to-paddle area ratio, chip-to-package area ratio, chip-to-paddle width ratio, etc.) and *fracture* criteria (such as fracture toughness of the molding compound, or the interfacial energy release rate).

The obtained constitutive equations account for the following major factors:

(1) Nonuniform distribution of temperature in the molding compound in the in-plane and the through-thickness directions.

(2) Temperature dependence of Young's modulus and the coefficient of expansion of the compound (note that such a dependence, in combination with temperature gradients, makes the material anisotropic).

(3) Thermally induced stresses caused by the thermal expansion mismatch of the dissimilar materials in the package.

(4) Thermally induced stresses due to the thermal expansion mismatch of the materials.

(5) Initial stresses and initial curvature (if any).

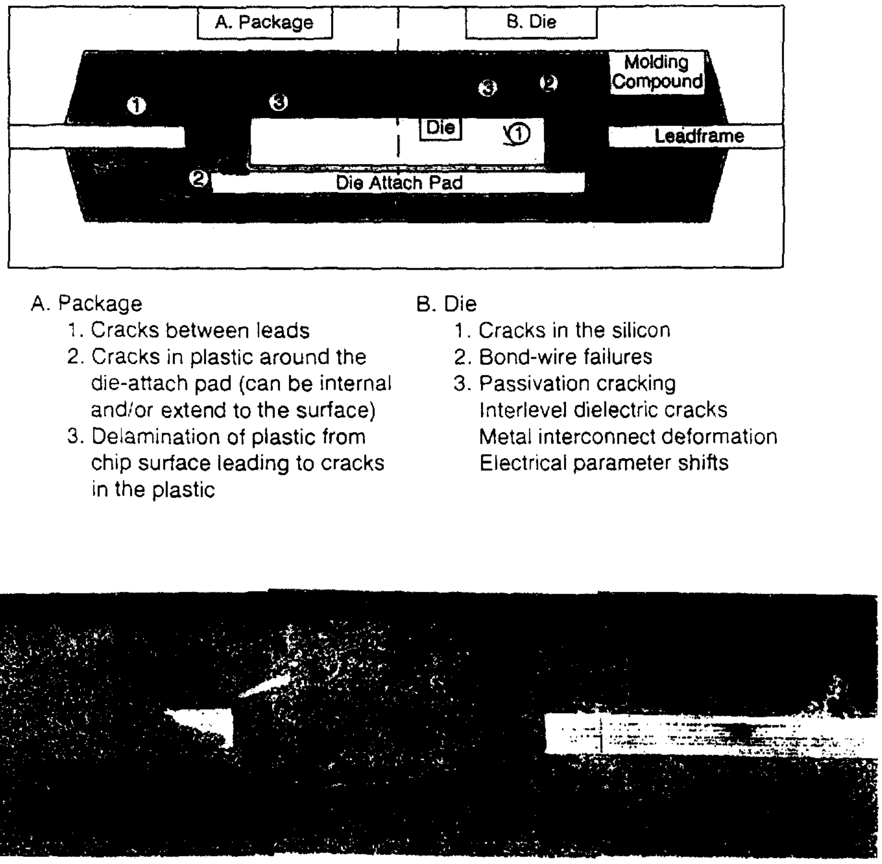

Fig. 1. Moisture-induced failures in a typical plastic package. The portion of the molding compound below the pad or above the chip can be treated, from the viewpoint of structural analysis, as a rectangular plate clamped on the support contour.

ANALYSIS

Constitutive equations

The von-Kármán equations (see, e.g., Timoshenko and Woinowski-Krieger, 1959) for large deflections of rectangular plates (Fig. 2) can be generalized to account for the thermoelastic strains, and the initial stresses and curvature as follows (Suhir, 1995):

$$\left.\begin{aligned} D\nabla^4 w + L_D(D, w) &= hL(w+\bar{w}, \phi) + p + \nabla^2 M_T - \bar{\sigma}_x^0 \frac{\partial^2 w}{\partial x^2} - \bar{\sigma}_y^0 \frac{\partial^2 w}{\partial y^2} - 2\bar{\tau}_{xy}^0 \frac{\partial^2 w}{\partial x\,\partial y} \\ C\nabla^4 w + L_C(C, \phi) &= -\frac{1}{2h} L(w+2\bar{w}, w) - \frac{1-v}{h}\nabla^2 (CN_T) \end{aligned}\right\}. \tag{1}$$

Here, $w(x, y)$ is the deflection function (vertical displacements of the points located in the *main plane*, $z = 0$, placed at the distance

$$z_C = \frac{\int_0^h E z_1 \,\mathrm{d}z_1}{\int_0^h E \,\mathrm{d}z_1} \tag{2}$$

from the lower surface of the plate), $E = E[T(x, y, z)]$ is (temperature dependent) Young's modulus of the plate's materials, $T = T(x, y, z)$ is the temperature at the arbitrary point (x, y, z) of the plate, $z_1 = z + z_C$ is the distance of this point from the lower surface of the plate (in the case of a plastic package, the distance z_1 is counted from the outer surface of the package), h is the plate's thickness (in the case of a plastic package, the *underchip thickness* of the molding compound, i.e., the thickness of the molding compound layer between its interface with the chip or the paddle and the outer surface of the package), $\phi = \phi(x, y)$ is the Airy (stress) function related to the in-plane ("membrane") stresses acting in the x–y plane by the formulae

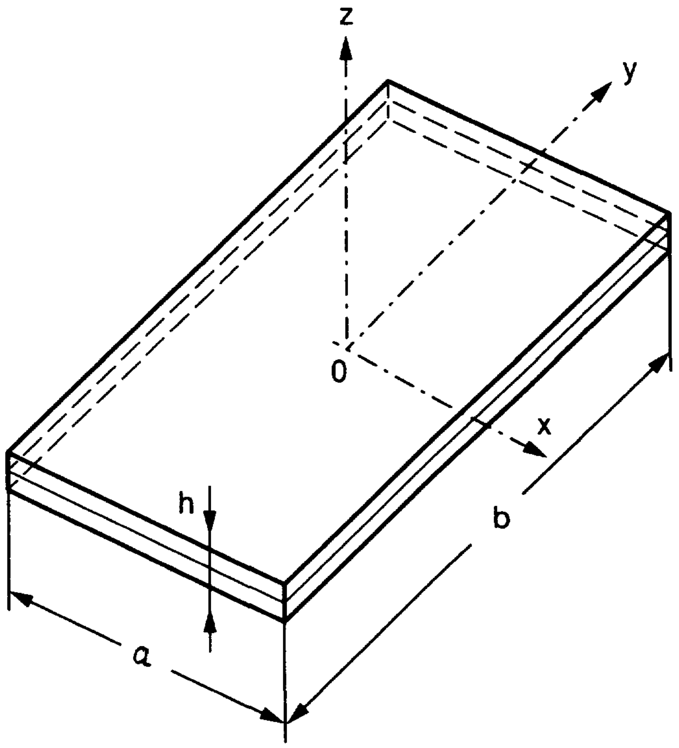

Fig. 2. Plate dimensions.

$$\sigma_x^0 = \frac{\partial^2 \phi}{\partial y^2}, \quad \sigma_y^0 = \frac{\partial^2 \phi}{\partial x^2}, \quad \tau_{xy}^0 = -\frac{\partial^2 \phi}{\partial x \, \partial y}, \tag{3}$$

$\sigma_x^0 = \sigma_x^0(x,y,z)$ and $\sigma_y^0 = \sigma_y^0(x,y,z)$ are the in-plane ("membrane") normal stresses in the directions x and y, respectively, $\tau_{xy}^0 = \tau_{xy}^0(x,y,z)$ is the shearing in-plane stress, $\bar{\sigma}_x^0$ and $\bar{\sigma}_y^0$ are the initial values of the normal in-plane stresses, $\bar{\tau}_{xy}^0$ is the initial value of the shearing in-plane stress, $p \equiv p(x,y)$ is the lateral load acting on the plate (in the case of a plastic package, it is the lateral water vapor induced pressure),

$$D = D(x,y) = \frac{1}{1-\nu^2}\int_{-z_c}^{h-z_c} Ez^2 \, \mathrm{d}z = \frac{E_D h^3}{12(1-\nu^2)} \tag{4}$$

is the flexural rigidity of the plate (molding compound layer)

$$E_D = \frac{12}{h^3}\int_{-z_c}^{h-z_c} Ez^2 \, \mathrm{d}z \tag{5}$$

is the effective Young's modulus with respect to bending deformations, ν is Poisson's ratio of the plate's material (in this study this ratio is considered constant, i.e., temperature independent),

$$C = C(x,y) = \left(\int_{-z_c}^{h-z_c} E \, \mathrm{d}z\right)^{-1} \tag{6}$$

is the in-plane compliance of the plate (molding compound layer),

$$\nabla^2 = \Delta = \frac{\partial^2}{\partial x^2} + \frac{\partial^2}{\partial y^2}$$

is the Laplace operator,

$$\nabla^4 = \nabla^2\nabla^2 = \Delta\Delta = \frac{\partial^4}{\partial x^4} + 2\frac{\partial^4}{\partial x^2 \, \partial y^2} + \frac{\partial^4}{\partial y^2}$$

is the biharmonic operator, the operator L is expressed as

$$L(w,\phi) = \frac{\partial^2 w}{\partial x^2}\frac{\partial^2 \phi}{\partial y^2} - 2\frac{\partial^2 w}{\partial x \, \partial y}\frac{\partial^2 \phi}{\partial x \, \partial y} + \frac{\partial^2 w}{\partial y^2}\frac{\partial^2 \phi}{\partial x^2},$$

so that

$$L(w+2\bar{w}, w) = 2\left[\frac{\partial^2 w}{\partial x^2}\frac{\partial^2 w}{\partial y^2} - \left(\frac{\partial^2 w}{\partial x \, \partial y}\right)^2 + \frac{\partial^2 w}{\partial x^2}\frac{\partial^2 \bar{w}}{\partial y^2} - \frac{\partial^2 w}{\partial x \, \partial y}\frac{\partial^2 \bar{w}}{\partial x \, \partial y} + \frac{\partial^2 w}{\partial y^2}\frac{\partial^2 \bar{w}}{\partial x^2}\right],$$

the operators L_D and L_C are expressed as

$$L_D = L_D(D, w) = \left(\frac{\partial^2 D}{\partial x^2} + v\frac{\partial^2 D}{\partial y^2}\right)\frac{\partial^2 w}{\partial x^2} + \left(\frac{\partial^2 D}{\partial y^2} + v\frac{\partial^2 D}{\partial x^2}\right)\frac{\partial^2 w}{\partial y^2}$$

$$+2\left[\frac{\partial D}{\partial x}\frac{\partial \nabla^2 w}{\partial x} + (1-v)\frac{\partial^2 D}{\partial x\,\partial y}\frac{\partial^2 w}{\partial x\,\partial y} + \frac{\partial D}{\partial y}\frac{\partial \nabla^2 w}{\partial y}\right],$$

and

$$L_C = L_C(C, \phi) = \left(\frac{\partial^2 C}{\partial x^2} - v\frac{\partial^2 C}{\partial y^2}\right)\frac{\partial^2 \phi}{\partial x^2} + \left(\frac{\partial^2 C}{\partial y^2} - v\frac{\partial^2 C}{\partial x^2}\right)\frac{\partial^2 \phi}{\partial y^2}$$

$$+2\left[\frac{\partial C}{\partial x}\frac{\partial \nabla^2 \phi}{\partial x} + (1+v)\frac{\partial^2 C}{\partial x\,\partial y}\frac{\partial^2 \phi}{\partial x\,\partial y} + \frac{\partial C}{\partial y}\frac{\partial \nabla^2 \phi}{\partial y}\right]$$

(note that the only difference between the operators L_D and L_C is the sign in front of Poisson's ratio v),

$$N_T = \frac{1}{1-v}\int_{-z_c}^{h-z_c} E\alpha\,\Delta T\,\mathrm{d}z, \quad M_T = \frac{1}{1-v}\int_{-z_c}^{h-z_c} E\alpha\,\Delta T z\,\mathrm{d}z \tag{7}$$

are the thermally induced in-plane force and the bending moment, respectively, $\alpha \equiv \alpha[T(x,y,z)]$ is the (temperature dependent) coefficient of thermal expansion of the material, and $\Delta T = \Delta T(x,y,z)$ is the change in temperature at the point (x,y,z). The origin O of the rectangular coordinates x, y, z is in the center of the main plane.

Boundary conditions

The boundary conditions for the deflection function $w(x,y)$ of a plate clamped around its contour are as follows:

$$\left.\begin{aligned} &w = 0, \quad \text{for } x = \pm\frac{a}{2}, y = \pm\frac{b}{2};\\ &\frac{\partial w}{\partial x} = 0, \quad \text{for } x = \pm\frac{a}{2};\\ &\frac{\partial w}{\partial y} = 0, \quad \text{for } y = \pm\frac{b}{2} \end{aligned}\right\}. \tag{8}$$

Here, a is the dimension of the plate along the x axis, and b is its dimension along the y axis.

If the plate's support contour is nondeformable (i.e., if the plate's edges cannot move closer during the plate's deformation), the plate will experience in-plane ("membrane") stresses. These stresses should satisfy the following conditions of the nondeformability of the support contour (see, e.g., Suhir, 1991):

$$\left.\begin{aligned} \int_0^{a/2}\frac{1}{E_C}(\sigma_x^0 - v\sigma_y^0)\,\mathrm{d}x &= \int_0^{a/2}\frac{1}{E_C}\left(\frac{\partial^2\phi}{\partial y^2} - v\frac{\partial^2\phi}{\partial x^2}\right)\mathrm{d}x = \frac{1}{2}\int_0^{a/2}\left(\frac{\partial w}{\partial x}\right)^2\mathrm{d}x\\ \int_0^{b/2}\frac{1}{E_C}(\sigma_y^0 - v\sigma_x^0)\,\mathrm{d}y &= \int_0^{b/2}\frac{1}{E_C}\left(\frac{\partial^2\phi}{\partial x^2} - v\frac{\partial^2\phi}{\partial y^2}\right)\mathrm{d}y = \frac{1}{2}\int_0^{b/2}\left(\frac{\partial w}{\partial y}\right)^2\mathrm{d}y \end{aligned}\right\}, \tag{9}$$

where

$$E_C = \frac{1}{h}\int_{-z_c}^{h-z_c} E\,\mathrm{d}z = \frac{1}{h}\int_0^h E\,\mathrm{d}z_1 \tag{10}$$

is the effective Young's modulus of the material with respect to in-plane tension or compression.

Stresses

After eqns (1), with the boundary conditions (8) and the conditions (9) of the non-deformability of the plate's contour, are solved, the induced stresses in the molding compound can be evaluated by the formulae (Suhir, 1995):

$$\left.\begin{aligned} \sigma_x &= E\left[C(N_x+N_T)-z\frac{M_x-M_T}{(1-\nu^2)D}-\frac{\alpha\Delta T}{1-\nu}\right] \\ \sigma_y &= E\left[C(N_y+N_T)-z\frac{M_y-M_T}{(1-\nu^2)D}-\frac{\alpha\Delta T}{1-\nu}\right] \\ \tau_{xy} &= E\left[CN_{xy}-z\frac{M_{xy}}{(1-\nu^2)D}\right] \end{aligned}\right\}, \tag{11}$$

where

$$\left.\begin{aligned} M_x &= D\left(\frac{\partial^2 w}{\partial x^2}+\nu\frac{\partial^2 w}{\partial y^2}\right)+M_T \\ M_y &= D\left(\frac{\partial^2 w}{\partial y^2}+\nu\frac{\partial^2 w}{\partial x^2}\right)+M_T \\ M_{xy} &= D(1-\nu)\frac{\partial^2 w}{\partial x\,\partial y} \end{aligned}\right\} \tag{12}$$

are the bending moments with respect to the axes, x, y, and z, respectively, and

$$N_x = h\frac{\partial^2\phi}{\partial y^2} = h\sigma_x^0,\quad N_y = h\frac{\partial^2\phi}{\partial x^2} = h\sigma_y^0,\quad N_{xy} = -h\frac{\partial^2\phi}{\partial x\,\partial y} = h\tau_{xy}^0 \tag{13}$$

are the in-plane forces.

Special cases

Examine several special cases for eqns (1).

(1) The effect of the temperature gradient on the change in Young's modulus in the x–y plane is small.

In this case, the flexural rigidity, D, and the in-plane compliance, C, expressed by the formulae (4) and (6), respectively, are independent of the coordinates x and y, and eqns (1) can be simplified:

$$\left.\begin{aligned} D\nabla^4 w &= hL(w+\bar{w},\phi)+p+\nabla^2 M_T-\bar{\sigma}_x^0\frac{\partial^2 w}{\partial x^2}-\bar{\sigma}_y^0\frac{\partial^2 w}{\partial y^2}-2\bar{\tau}_{xy}^0\frac{\partial^2 w}{\partial x\,\partial y}, \\ C\nabla^4\phi &= -\frac{1}{2h}L(w+2\bar{w},w)-\frac{1-\nu}{h}\nabla^2(CN_T) \end{aligned}\right\}. \tag{14}$$

If, in addition, there is no initial curvature ($w = 0$), nor the initial in-plane stresses ($\bar{\sigma}_x^0 = \bar{\sigma}_y^0 = \bar{\tau}_{xy}^0 = 0$), then eqns (14) can be further simplified:

$$\left.\begin{aligned} D\nabla^4 w &= hL(w_1\phi)+p+\nabla^2 M_T \\ C\nabla^4\phi &= -\frac{1}{2h}L(w,w)-\frac{1-v}{h}\nabla^2(CN_T) \end{aligned}\right\}. \tag{15}$$

(2) The temperature changes in the through-thickness direction only.

If the temperature gradient in the x–y plane is zero and, in addition, no initial deflections nor initial stresses occur, then the last terms in eqns (15) are zero as well, so that

$$D\nabla^4 w = hL(w,\phi)+p, \quad C\nabla^4\phi = -\frac{1}{2h}L(w,w). \tag{16}$$

These equations are not different from the "conventional" von-Kármán equations for large deflections of rectangular plates subjected to a distributed lateral load (Timoshenko and Woinowski-Krieger, 1959). The only difference is in how the flexural rigidity D and the in-plane compliance C are computed. These should be evaluated by the formulae (4) and (6), i.e., with consideration of the change in Young's modulus in the through-thickness direction as a function of temperature.

(3) The lateral pressure is zero, and the plates edges cannot move in its plane.

In this case, $N_x = N_y = -N_T$, the bending moments are zero everywhere, and, in the absence of the initial stresses and curvatures, the formulae (11) yield:

$$\sigma_x = \sigma_y = E\left[z\frac{M_T}{(1-v^2)D}-\frac{\alpha\Delta T}{1-v}\right]. \tag{17}$$

(4) The lateral pressure is zero and the plate is free of supports.

In this case, $N_x = N_y = N_{xy} = 0$, $M_x = M_y = M_{xy} = 0$, and, if the initial stresses and curvatures are zero as well, the formulae (1) yield $\tau_{xy} = 0$, so that

$$\sigma_x = \sigma_y = E\left[CN_T+z\frac{M_T}{(1-v^2)D}-\frac{\alpha\Delta T}{1-v}\right]. \tag{18}$$

The deflections in such a plate were examined in detail in Suhir (1993) in application to thermally induced bowing of plastic packages.

(5) The lateral pressure is zero, the plate's edges are clamped, and the temperature changes in the through-thickness direction only.

In this case, $N_x = N_y = -N_T$, $M_x = M_y = M_T$, and, if there are no initial stresses nor forces, the formulae (11) yield:

$$\sigma_x = \sigma_y = -\frac{E\alpha\Delta T}{1-v}. \tag{19}$$

This formula indicates that the plate remains flat and experiences in-plane normal stresses only.

Initial curvature and initial stresses

The initial temperature-induced curvature and the initial stresses can be determined, if there is a need for that, on the basis of a simplified analysis that is set forth below.

Let the plastic package be subjected to a uniform change ΔT in temperature. The thermally induced forces, F_i, $i = 1, 2, 3, 4$, acting in the constituent materials, and the thermally induced curvature of the composite structure (Fig. 3), can be evaluated, assuming perfect adhesion, from the

(1) strain compatibility conditions:

$$\left.\begin{aligned}-\alpha_1\,\Delta T+C_1F_1+\frac{h_1}{2}\kappa_0 &= -\alpha_2\,\Delta T+C_2F_2-\frac{h_2}{2}\kappa_0\\ -\alpha_2\,\Delta T+C_2F_2+\frac{h_2}{2}\kappa_0 &= -\alpha_3\,\Delta T+C_3F_3-\frac{h_3}{2}\kappa_0\\ -\alpha_3\,\Delta T+C_3F_3+\frac{h_3}{2}\kappa_0 &= -\alpha_1\,\Delta T+C_4F_4-\frac{h_4}{2}\kappa_0\end{aligned}\right\}, \tag{20}$$

(2) equilibrium equation for the induced forces:

$$F_1+F_2+F_3+F_4 = 0, \tag{21}$$

(3) equilibrium equation for the induced bending moments:

$$\left(\frac{h_1}{2}+h_2+h_3+\frac{h_4}{2}\right)F_1+\left(\frac{h_2}{2}+h_3+\frac{h_4}{2}\right)F_2+\left(\frac{h_3}{2}+\frac{h_4}{2}\right)F_3 = EI\kappa_0. \tag{22}$$

In these equations, α_1, α_2 and α_3 are the thermal expansion coefficients for the molding compound, the metal paddle, and the silicon chip, respectively,

$$C_i = \frac{1-\nu_i}{E_ih_i}, \quad i = 1,2,3,4, \tag{23}$$

are the in-plane compliances of the materials layers, E_i and ν_i, $i = 1, 2, 3$, are elastic constants of the materials, h_i, $i = 1, 2, 3, 4$ are the layers' thicknesses, κ_0 is the temperature induced curvature of the molding body, and EI is its flexural rigidity.

The first terms in either part of the conditions (20) are unrestricted ("stress free") thermal contractions. The second terms are the strains due to the thermally induced forces. The third terms are due to bending. Clearly, the bending strains have opposite signs on the convex and the concave sides of the given layer.

Equations (20) are written assuming that the curing temperature of the attachment of the chip to the paddle is the same as the molding temperature, so that the temperature change ΔT can be considered the same throughout the molding body. Equation (21) states that, since no other forces but the thermally induced ones act on the package, the thermal forces must be self-equilibrated. As to the equilibrium equation for the bending moments,

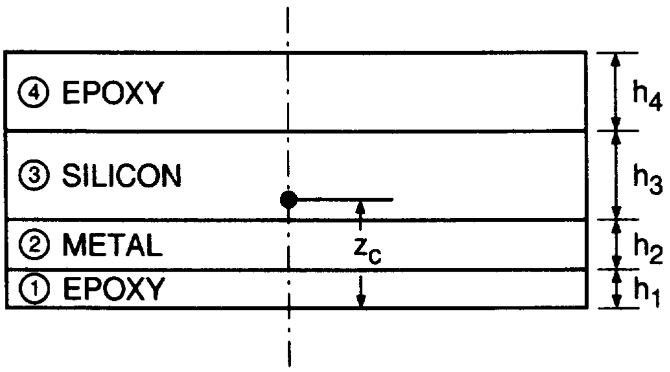

Fig. 3. Cross-section of a plastic package.

this can be formed with respect to any horizontal axis located in the plane of the given cross-section. In our analysis, this equation is written with respect to the midplane of the fourth ($i = 4$) layer. This led to eqn (22).

Equations (20)–(22) can be rewritten as

$$\left.\begin{aligned} C_1F_1 - C_2F_2 + \beta_{12}\kappa_0 &= \alpha_{12}\,\Delta T \\ C_2F_2 - C_3F_3 + \beta_{23}\kappa_0 &= \alpha_{23}\,\Delta T \\ C_3F_3 - C_4F_4 + \beta_{34}\kappa_0 &= \alpha_{13}\,\Delta T \\ F_1 + F_2 + F_3 + F_4 &= 0 \\ \beta_{14}F_1 + \beta_{24}F_2 + \beta_{34}F_3 - EI\kappa_0 &= 0 \end{aligned}\right\}, \tag{24}$$

where the following notation is used:

$$\left.\begin{aligned} &\alpha_{12} = \alpha_1 - \alpha_2, \quad \alpha_{23} = \alpha_2 - \alpha_3, \quad \alpha_{13} = \alpha_1 - \alpha_3 \\ &\beta_{12} = \frac{h_1 + h_2}{2}, \quad \beta_{23} = \frac{h_2 + h_3}{2}, \quad \beta_{34} = \frac{h_3 + h_4}{2}, \\ &\beta_{14} = \beta_{12} + \beta_{23} + \beta_{34}, \quad \beta_{24} = \beta_{23} + \beta_{34} \end{aligned}\right\}. \tag{25}$$

Equations (24) have the following solution:

$$\left.\begin{aligned} F_1 &= \frac{\Delta T}{D}\{\alpha_{12}[(C_2C_3 + C_3C_4 + C_2C_4)EI + C_2\beta_{34}^2 + C_3\beta_{24}^2 + C_4\beta_{23}^2] \\ &\quad + \alpha_{23}[C_2(C_3 + C_4)EI + C_2\beta_{34}^2 - C_3\beta_{12}\beta_{24} - C_4\beta_{12}\beta_{23}] \\ &\quad + \alpha_{13}(C_2C_3EI - C_2\beta_{23}\beta_{34} - C_3\beta_{12}\beta_{24})\} \\ F_2 &= \frac{\Delta T}{D}\{-\alpha_{12}(C_3C_4EI + C_3\beta_{14}\beta_{24} + C_4\beta_{13}\beta_{23}) \\ &\quad + \alpha_{23}[C_1(C_3 + C_4)EI + C_1\beta_{34}^2 + C_3\beta_{12}\beta_{14} + C_4\beta_{12}\beta_{13}] \\ &\quad + \alpha_{13}(C_1C_3EI - C_1\beta_{23}\beta_{34} + C_3\beta_{12}\beta_{14})\} \\ F_3 &= \frac{\Delta T}{D}\{-\alpha_{12}(C_2C_4EI + C_2\beta_{14}\beta_{34} - C_4\beta_{12}\beta_{23}) \\ &\quad - \alpha_{23}[C_4(C_1 + C_2)EI + C_1\beta_{24}\beta_{34} + C_2\beta_{14}\beta_{34} + C_4\beta_{12}^2] \\ &\quad + \alpha_{13}(C_1C_2EI + C_1\beta_{23}\beta_{24} + C_2\beta_{13}\beta_{14})\} \\ F_4 &= -\frac{\Delta T}{D}\{\alpha_{12}(C_2C_3EI - C_2\beta_{13}\beta_{34} - C_3\beta_{12}\beta_{24}) \\ &\quad + \alpha_{23}[C_3(C_1 + C_2)EI - C_1\beta_{23}\beta_{34} - C_2\beta_{13}\beta_{34} + C_3\beta_{12}^2] \\ &\quad + \alpha_{13}[(C_1C_2 + C_1C_3 + C_2C_3)EI + C_1\beta_{23}^2 + C_2\beta_{13}^2 + C_3\beta_{12}^2]\} \\ \kappa_0 &= -\frac{\Delta T}{D}\{\alpha_{12}(C_2C_4\beta_{13} + C_3C_4\beta_{12} + C_2C_3\beta_{34}) \\ &\quad + \alpha_{23}(C_1C_4\beta_{23} + C_1C_3\beta_{24} + C_2C_3\beta_{14} + C_2C_4\beta_{34}) \\ &\quad + \alpha_{13}(C_1C_2\beta_{34} + C_1C_3\beta_{24} + C_2C_3\beta_{14})\}, \end{aligned}\right\} \tag{26}$$

where

$$D = EIC + C_1C_2\beta_{34}^2 + C_1C_3\beta_{24}^2 + C_1C_4\beta_{23}^2 + C_2C_4\beta_{13}^2 + C_2C_3\beta_{14}^2 + C_3C_4\beta_{12}^2$$

is the determinant of eqns (24), and

$$C = C_1C_2C_3 + C_1C_2C_4 + C_1C_3C_4 + C_2C_3C_4.$$

In order to determine the deflection function from the obtained curvature, we use the following equation for the curvature of the composite plate:

$$\frac{\partial^2 w}{\partial x^2} = \frac{\partial^2 w}{\partial y^2} = -\kappa_0.$$

After integration, we obtain:

$$w = w_0 - \tfrac{1}{2}\kappa_0(x^2 + y^2),$$

where w_0 is the deflection at the center of the plate. For a rectangular package, the maximum bow can be determined from the condition

$$w\left(\frac{a}{2}, \frac{b}{2}\right) = 0,$$

where a and b are the plate sides. This results in the following formula for the maximum bow:

$$w_0 = \frac{a^2 + b^2}{8}\kappa_0. \tag{27}$$

The equation for the initially deflected surface of the package can be written as

$$\bar{w} = \frac{1}{2}\kappa_0\left[\left(\frac{a}{2}\right)^2 - x^2 + \left(\frac{b}{2}\right)^2 - y^2\right], \tag{28}$$

and the initial in-plane stresses can be evaluated by the formula:

$$\sigma_i^0 = \frac{F_i}{h_i}, \quad i = 1, 2, 3, 4. \tag{29}$$

As to the initial bending stresses, they can be determined from the computed curvature κ_0 by the formulae

$$\sigma_1 = \frac{E_1\kappa_0}{6(1-\nu_1)}h_1^2, \quad \sigma_2 = \frac{E_2\kappa_0}{6(1-\nu_2)}h_2^2, \quad \sigma_3 = \frac{E_3\kappa_0}{6(1-\nu_3)}h_3^2, \quad \sigma_4 = \frac{E_1\kappa_0}{6(1-\nu_1)}h_4^2. \tag{30}$$

Elongated package

Elastic curve. In this section we examine a special case of eqns (14), when the plate, experiencing large deflections, is characterized by a sufficiently high aspect ratio (the b/a ratio is larger than, say, 2.5), so that it can be treated as an elongated plate. If this is the case, the solution to eqns (14) can be simplified significantly. At the same time, the solution obtained for an elongated plate will be conservative, i.e., will result in a reasonable overestimation of the induced deflections and stresses.

In the case of an elongated plate, one can consider a relatively simple problem of bending of a strip oriented along the x axis, i.e., along the plate's width. The equation of bending of such a strip can be written as follows:

$$D\frac{\partial^2 w}{\partial x^4} - F\frac{\partial^2 w}{\partial x^2} = p. \tag{31}$$

Here, $w = w(x)$ is the deflection function,

$$D = \frac{Eh^3}{12(1-v^2)}$$

is the flexural rigidity of the plate, h is its thickness, E and v are the elastic constants of the material, F is the tensile force, and p is the distributed load. In this analysis it is assumed that the load p is constant within the interval $-c/2 \leqslant x \leqslant c/2$, and is equal to zero outside this interval. The origin O of the coordinate x is in the middle of the plate at its neutral plane.

Equation (31) can be rewritten as

$$\frac{\partial^4 w}{\partial x^4} - k^2 \frac{\partial^2 w}{\partial x^2} = \frac{p}{D}, \tag{32}$$

where

$$k = \sqrt{\frac{F}{D}} \tag{33}$$

is the eigenvalue of the problem.

Because of the stress relaxation, the curvature of, and the stresses in the plastic package at room temperature (prior to reflow soldering) can be different from the residual bow and residual stresses in a newly fabricated package. If this is indeed the case, the package will not be flat and the stresses in it will not be zero at the reflow soldering temperature. In such a situation the initial curvature at room temperature can be measured, and then the last formula in (26) can be used to determine the $\Delta T/D$ ratio. After substituting this ratio into the first four formulae in (26), one can determine the induced forces. The initial in-plane stresses can be then computed on the basis of formulae (29), and the bending stresses can be determined by formulae (30).

The solution to eqn (32) can be sought, for the interval $-c/2 \leqslant x \leqslant c/2$, as

$$w(x) = C_0 + C_1 \cosh kx - \frac{px^2}{2F}, \tag{34}$$

where C_0 and C_1 are the constants of integration. In expression (34), it is taken into account that the deflections $w(x)$ must be symmetric with respect to the origin, and therefore only the even functions should be considered.

From (34) we find:

$$\left.\begin{aligned} w\left(\frac{c}{2}\right) &= C_0 + C_1 \cosh\frac{kc}{2} + \frac{pc^2}{8F} \\ w'\left(\frac{c}{2}\right) &= kC_1 \sinh\frac{kc}{2} - \frac{pc}{2F} \\ w''\left(\frac{c}{2}\right) &= k^2 C_1 \cosh\frac{kc}{2} - \frac{p}{F} \\ w'''\left(\frac{c}{2}\right) &= k^3 C_1 \sinh\frac{kc}{2} \end{aligned}\right\}. \tag{35}$$

The solution to eqn (34) outside the interval $-c/2 \leqslant x \leqslant c/2$ is

$$w_1(x_1) = C_2 + C_3 k x_1 + C_4 \cosh k x_1 + C_5 \sinh k x_1, \tag{36}$$

where $x_1 = x-(c/2)$. From (36) we obtain:

$$\left.\begin{array}{ll} w_1(0) = C_2 + C_4, & w_1'(0) = kC_3 + kC_5 \\ w_1''(0) = k^2 C_4, & w_1'''(0) = k^3 C_5 \end{array}\right\}. \tag{37}$$

The compatibility conditions for the displacements, angles of rotation, bending moments (curvatures), and lateral forces require that the following relationships take place:

$$w\left(\frac{c}{2}\right) = w_1(0); \quad w'\left(\frac{c}{2}\right) = w_1'(0); \quad w''\left(\frac{c}{2}\right) = w_1''(0); \quad w'''\left(\frac{c}{2}\right) = w_1'''(0). \tag{38}$$

Introducing the formulae (35) and (37) into the compatibility conditions (38), we obtain the following equations for the unknown constants of integration:

$$\left.\begin{array}{l} C_0 + C_1 \cosh\frac{kc}{2} + C_2 - C_4 = \frac{pc^2}{8F} \\ C_1 \sinh\frac{kc}{2} - C_3 - C_5 = \frac{pc}{2kF} \\ C_1 \cosh\frac{kc}{2} - C_4 = \frac{p}{k^2 F} \\ C_1 \sinh\frac{kc}{2} - C_5 = 0 \end{array}\right\}. \tag{39}$$

In addition to the compatibility conditions (38), the solution (36) must satisfy also the boundary conditions at the plate's ends:

$$w_1\left(\frac{a-c}{2}\right) = 0, \quad w_1'\left(\frac{a-c}{2}\right) = 0. \tag{40}$$

These conditions indicate that both the deflection and the rotation angle must be zero at the clamped edges. The four eqns (39) and the two conditions (40) enable one to determine the six constants of integration C_i, $i = 0, 1, 2, 3, 4, 5$:

$$C_0 = -\frac{p}{k^2 F}\left[1 - \frac{1}{2}\left(\frac{kc}{2}\right)^2\left(2\frac{a}{c} - 1\right) - \frac{\sinh\frac{kc}{2}}{\sinh\frac{ka}{2}} + \frac{kc}{2}\operatorname{cotanh}\frac{ka}{2}\right], \tag{41}$$

$$C_1 = \frac{p}{k^2 F}\,\frac{\sinh\frac{k(a-c)}{2} + \frac{kc}{2}}{\sinh\frac{ka}{2}}, \tag{42}$$

$$C_2 = \frac{p}{k^2 F}\left[\left(\frac{kc}{2}\right)^2\left(\frac{a}{c} - 1\right) + \frac{\sinh\frac{kc}{2}}{\sinh\frac{ka}{2}} - \frac{kc}{2}\operatorname{cotanh}\frac{ka}{2}\right], \tag{43}$$

$$C_3 = -\frac{pc}{2kF}, \tag{44}$$

$$C_4 = -\frac{p}{k^2F}\left[1-\cosh\frac{kc}{2}\frac{\sinh\frac{k(a-c)}{2}+\frac{kc}{2}}{\sinh\frac{ka}{2}}\right], \tag{45}$$

$$C_5 = \frac{p}{k^2F}\sinh\frac{kc}{2}\frac{\sinh\frac{k(a-c)}{2}+\frac{kc}{2}}{\sinh\frac{ka}{2}}. \tag{46}$$

After the constants of integration are evaluated, the maximum deflection f can be easily determined from (34) as follows:

$$f = w(0) = C_0+C_1 = w_0\chi_f\left(u,\frac{c}{a}\right). \tag{47}$$

Here

$$w_0 = \frac{pa^4}{384D} = \frac{1-v^2}{32E_D}p\frac{a^4}{h^3} \tag{48}$$

is the maximum deflection in the case of zero tensile force ($F = 0$) and a load distributed over the entire width a of the plate ($c = a$), the factor

$$\chi_f\left(u,\frac{c}{a}\right) = \frac{24}{u^4\sinh u}\left\{\left(u\frac{c}{a}\right)(1-\cosh u)+\sinh\left(u\frac{c}{a}\right)\right.$$
$$\left.+\sinh\left[u\left(1-\frac{c}{a}\right)\right]+\left[\frac{u^2}{2}\frac{c}{a}\left(2-\frac{c}{a}\right)-1\right]\sinh u\right\} \tag{49}$$

accounts for the effect of the finite width of the loaded area and the finite (nonzero) value of the tensile force, and the parameter u is

$$u = \frac{ka}{2} = \frac{a}{s}\sqrt{\frac{F}{D}}. \tag{50}$$

The factor χ_f is plotted in Fig. 4.

When there is no tensile load, applied to the plate ($F = 0, u = 0$), the formula (49) yields:

$$\chi_f = \frac{c}{a}\left(2-2\frac{c^2}{a^2}+\frac{c^3}{a^3}\right). \tag{51}$$

In another special case, when the lateral load is distributed over the entire plate's width ($c = a$), the formula (49) results in the expression

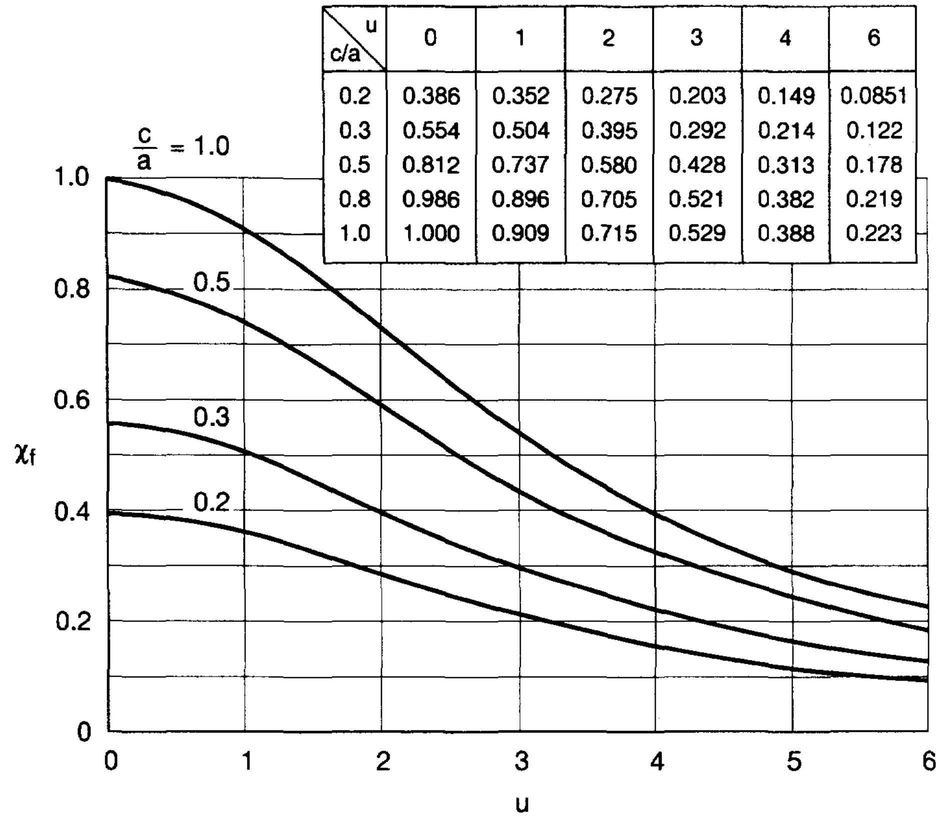

c/a \ u	0	1	2	3	4	6
0.2	0.386	0.352	0.275	0.203	0.149	0.0851
0.3	0.554	0.504	0.395	0.292	0.214	0.122
0.5	0.812	0.737	0.580	0.428	0.313	0.178
0.8	0.986	0.896	0.705	0.521	0.382	0.219
1.0	1.000	0.909	0.715	0.529	0.388	0.223

Fig. 4. Factor of the maximum deflection.

$$\chi_f = \frac{24}{u^3}\left(\frac{u}{2} - \tanh\frac{u}{2}\right). \tag{52}$$

Clearly, in the case $c = a$, the formula (51) yields $\chi_f = 1$, and so does the formula (52) in the case $u = 0$.

Bending stress. The bending stress at the clamped edge can be evaluated, using eqn (36) and the formulae (43) and (46) for the constants of integration, as follows:

$$\sigma_b = -\frac{E}{1-\nu^2}\frac{h}{2}w_1''\left(\frac{a-c}{2}\right) = \sigma_0\chi_M\left(u, \frac{c}{a}\right), \tag{53}$$

where

$$\sigma_0 = \frac{pa^2}{2h^2} \tag{54}$$

is the bending stress in the case of zero tensile force ($F = 0, u = 0$) and a load distributed over the entire width of the plate ($c = a$), and the factor

$$\chi_M\left(u, \frac{c}{a}\right) = \frac{3}{u^2}\frac{\left(u\frac{c}{a}\right)\cosh u - \sinh\left(u\frac{c}{a}\right)}{\sinh u} \tag{55}$$

considers the effect of the finite (nonzero) tensile force and the finite width of the loaded area on the bending moment (bending stress). This factor is plotted in Fig. 5. Note that the formula (53) is based on an assumption that the section modulus of the plate's cross-section can be evaluated as $h^2/6$, i.e., without considering the shift in the neutral plane due to the variable Young's modulus.

For a load, distributed over the entire width of the plate ($c = a$), the formula (55) yields:

$$\chi_M = \frac{3}{u^2}(u \operatorname{cotanh} u - 1). \tag{56}$$

In the absence of the tensile force ($F = 0, u = 0$), the relationship (55) leads to the following formula:

$$\chi_M = \frac{c}{2a}\left(3 - \frac{c^2}{a^2}\right). \tag{57}$$

Clearly, in the case $u = 0$, the formula (56) yields $\chi_M = 1$, and so does the formula (57) in the case of $c = a$.

When a concentrated lateral force is applied in the middle of the plate's width (span), formula (53) can be written as

$$\sigma_b = \sigma_0 \chi_1(u), \tag{58}$$

where

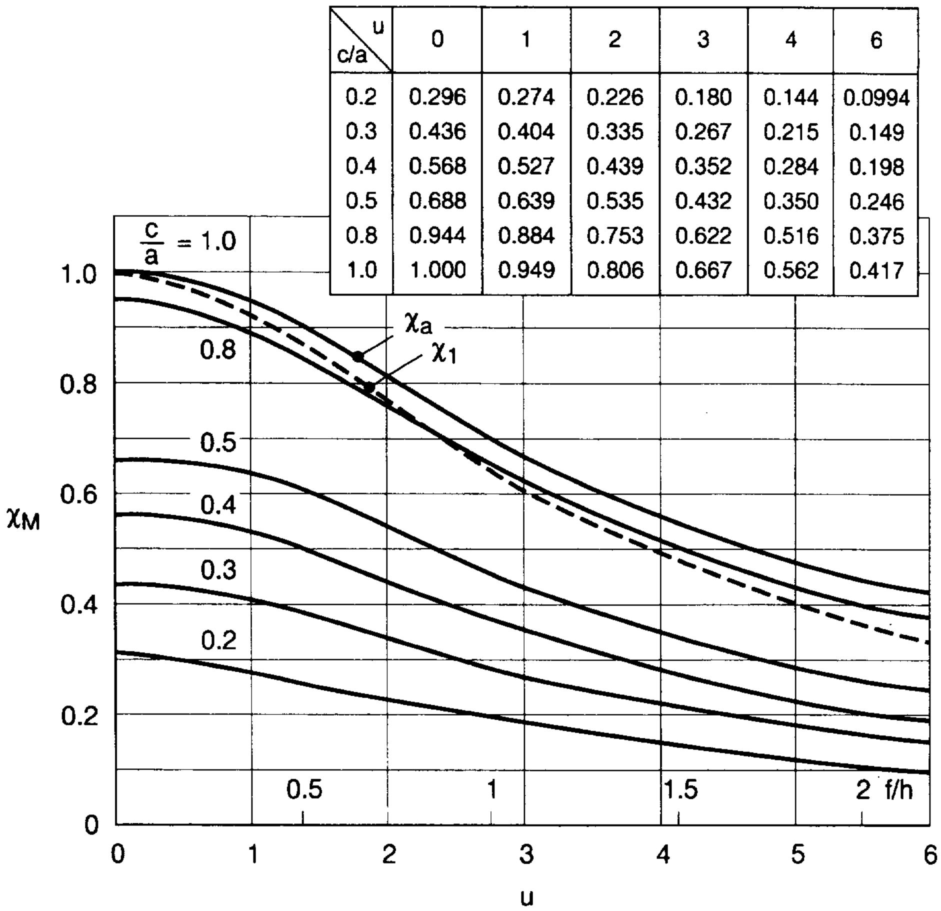

c/a \ u	0	1	2	3	4	6
0.2	0.296	0.274	0.226	0.180	0.144	0.0994
0.3	0.436	0.404	0.335	0.267	0.215	0.149
0.4	0.568	0.527	0.439	0.352	0.284	0.198
0.5	0.688	0.639	0.535	0.432	0.350	0.246
0.8	0.944	0.884	0.753	0.622	0.516	0.375
1.0	1.000	0.949	0.806	0.667	0.562	0.417

Fig. 5. Factor of the maximum bending moment.

$$\sigma_0 = \frac{3}{4}\frac{Pa}{h^2} = \frac{3}{4}\frac{pca}{h^2} \tag{59}$$

is the bending stress in the case when the tensile load is zero. The factor

$$\chi_1(u) = \frac{2}{u}\tanh u \tag{60}$$

reflects the effect of the finite (nonzero) force.

In-plane ("membrane") stress. The formulae that have been obtained in this section so far were derived for the given in-plane ("membrane") force F, i.e., assuming that the dimensionless parameter u, expressed by formula (50), is known. In the situation in question, however, the in-plane tensile force F depends on the deflection function $w(x)$ that, in its turn, depends on the magnitude of this force. Therefore an additional relationship between the unknown tensile force F and the unknown deflection function $w(x)$ is needed to determine the force F and the induced deflections. Such a relationship can be obtained from the biharmonic equation

$$\nabla^4 \phi = 0 \tag{61}$$

(this equation simply follows from the second equation in (16) in the case of an elongated plate for which the operator L is zero) and the conditions (9) of the nondeformability of the support contour.

In an approximate analysis, the solution to eqn (61) can be sought in the form

$$\phi = Ax^2 + By^2. \tag{62}$$

Then eqn (61) is fulfilled automatically, and the conditions (9) of the nondeformability of the contour, with $\partial w/\partial y = 0$ for $y = b/2$, yield:

$$A = \nu B = \frac{\nu E_c K}{4(1-\nu^2)}. \tag{63}$$

The expressions for the "mechanical" in-plane stresses caused by the lateral load p are

$$\bar{\sigma}_x^0 = \frac{\partial^2 \phi}{\partial y^2} = 2B = \frac{E_c K}{2(1-\nu^2)}, \quad \bar{\sigma}_y^0 = \frac{\partial^2 \phi}{\partial x^2} = 2A = \frac{\nu E_c K}{2(1-\nu^2)}, \tag{64}$$

where

$$K = \frac{2}{a}\int_0^{a/2} \left(\frac{\partial w}{\partial x}\right)^2 \mathrm{d}x. \tag{65}$$

Strictly speaking, the K value should be evaluated by introducing the solutions (34) and (36) into the integral in the formula (65) and by evaluating this integral as a sum of the integrals calculated separately for the intervals $0 \leqslant x \leqslant c/2$ and $0 \leqslant x \leqslant (a-c)/2$. Such a procedure leads, however, to tedious derivations and cumbersome relationships. At the same time, since the angle of rotation $\partial w/\partial x$ enters the formula (65) as an integrand, there is a reason to believe that even if an approximate configuration of the elastic curve is used, one can still obtain a sufficiently accurate K value.

Whatever the configuration, it should satisfy the boundary conditions (8) for a clamped plate. Using the expression

$$w(x) = f\left(1 - 8\frac{x^2}{a^2} + 16\frac{x^4}{a^4}\right)$$

for the elastic curve of a strip uniformly loaded over its length a (which is the width of the elongated plate) we obtain:

$$K = \frac{512}{105}\frac{f^2}{a^2} = 4.88\frac{f^2}{a^2}. \tag{66}$$

If the strip is loaded in its midcross-section by a concentrated force, then

$$w(x) = f\left(1 - 12\frac{x^2}{a^2} + 16\frac{x^4}{a^4}\right),$$

and the formula (65) yields:

$$K = \frac{24}{5}\frac{f^2}{a^2} = 4.80\frac{f^2}{a^2}. \tag{67}$$

If the deflection curve is approximated as

$$w(x) = f\cos^2\frac{\pi x}{a},$$

then

$$K = \frac{\pi^2}{2}\frac{f^2}{a^2} = 4.93\frac{f^2}{a^2}. \tag{68}$$

As one can see, the formulae (65), (66) and (67) give close results. It is natural to expect that for a plate partially loaded in its cross-section the coefficient in front of the (f/a) should be between the values obtained for the extreme cases of a distributed and a concentrated load:

$$K = \frac{1}{2}\left(\frac{512}{105} + \frac{24}{5}\right)\frac{f^2}{a^2} = \frac{508}{105}\frac{f^2}{a^2} = 4.84\frac{f^2}{a^2}. \tag{69}$$

Introducing (68) into the first equation in (64), we obtain the following relationship between the "mechanical" transverse in-plane stress and the deflection-to-width ratio:

$$\bar{\sigma}_x^0 = \frac{254}{105}\frac{E_c}{1-v^2}\frac{f^2}{a^2}. \tag{70}$$

Since the tensile force F can be evaluated as $F = \sigma_x^0 h$, the parameter u can be determined as

$$u = \frac{a}{2}\sqrt{\frac{\sigma_x^0 h}{D}} = \sqrt{\frac{254}{35}\frac{E_c}{E_D}\frac{f}{h}} = 2.694\sqrt{\frac{E_c}{E_D}\frac{f}{h}}. \tag{71}$$

This is the sought of the additional relationship between the tensile force and the maximum

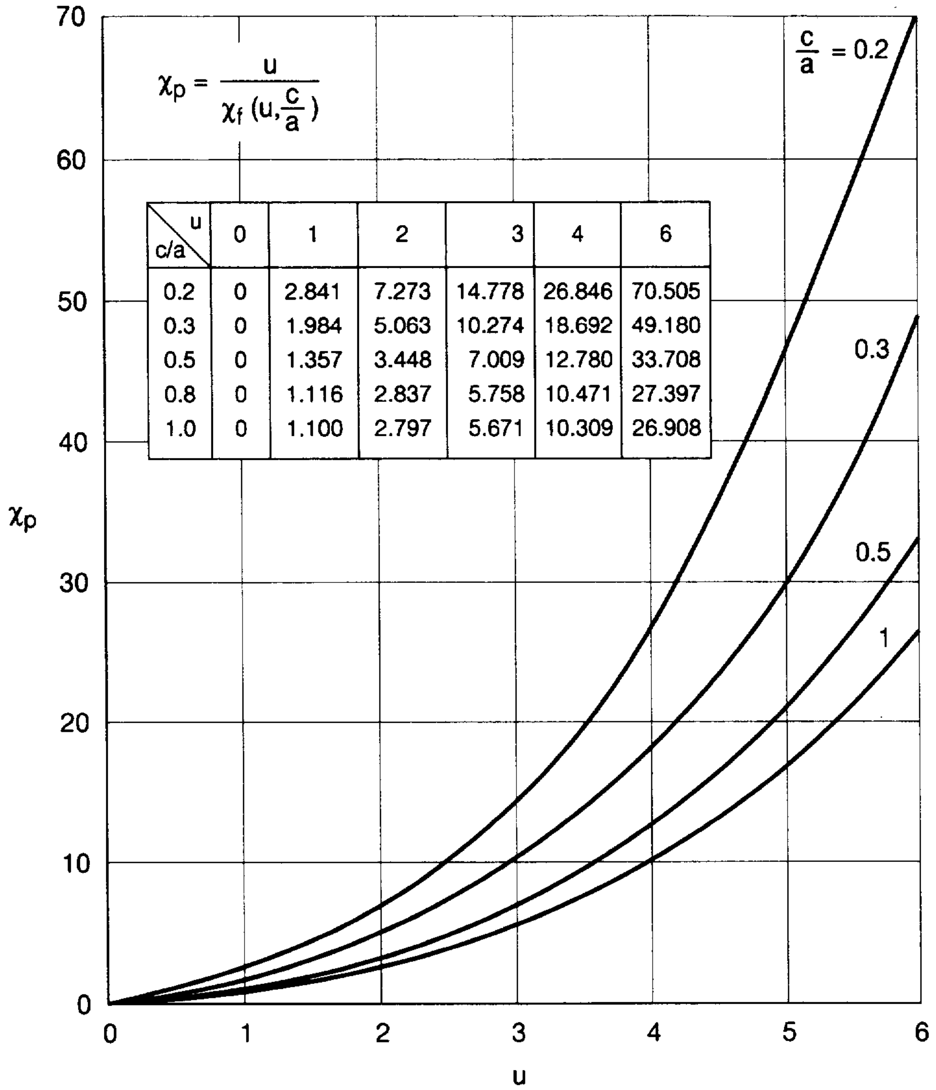

u / c/a	0	1	2	3	4	6
0.2	0	2.841	7.273	14.778	26.846	70.505
0.3	0	1.984	5.063	10.274	18.692	49.180
0.5	0	1.357	3.448	7.009	12.780	33.708
0.8	0	1.116	2.837	5.758	10.471	27.397
1.0	0	1.100	2.797	5.671	10.309	26.908

Fig. 6. Factor of the water vapor pressure.

deflection. After the nonlinear problem for the maximum deflection f is solved, the membrane stress $\tilde{\sigma}_x^0$ can be computed by the formula (69). The longitudinal in-plane stress $\tilde{\sigma}_y^0$ can be evaluated, as evident from (64), as $\tilde{\sigma}_y^0 = \nu\tilde{\sigma}_x^0$.

In order to simplify the computation of the maximum deflection f, one can use the following relationship which can be easily obtained from (48), (49) and (70):

$$\bar{p} = \frac{1-\nu^2}{32}\sqrt{\frac{254}{35}\frac{E_c}{E_D}}\left(\frac{a}{h}\right)^4\frac{p}{E_D} = \chi_p = \frac{u}{\chi_f}. \tag{72}$$

The relationship (71) is plotted in Fig. 6 and enables one to evaluate the parameter u from the computed dimensionless lateral load p. After the u value is determined, the deflection-to-thickness ratio f/h can be found from (70). Finally, the transverse stress $\tilde{\sigma}_x^0$ can be computed from the calculated maximum deflection by the formula (69). This formula can be written, considering (48), as

$$\tilde{\sigma}_x^0 = 0.002362(1-\nu^2)\frac{E_c}{E_D^2}p^2\left(\frac{a}{h}\right)^6\chi_f^2. \tag{73}$$

As evident from this formula, the in-plane ("membrane") stress can be quite large, if the lateral (water vapor) pressure p is appreciable and the ratio a/h is large. This is thought to be the case in thin small outline packages (TSOP's). In addition, it should be pointed out that the maximum bending stress, expressed by the formula (53), is rather weakly dependent on the Young modulus of the material. Indeed, Young modulus affects the bending stress only through the parameter u, and this parameter, as one can see from (70), is proportional, for the given deflection-to-thickness ratio, to the square root of the ratio of the effective Young's moduli in tension and in bending. As the calculations show, these Young's moduli are not much different. The in-plane ("membrane") stresses, however, are affected by the Young modulus of the material quite strongly: as evident from the formula (72), these stresses decrease with an increase in the Young modulus of the material. Therefore, one can conclude that when the lateral pressure is large and, as a consequence of that, the membrane stresses are substantial, molding compounds with higher Young's moduli are expected to result in lower induced stresses, i.e., be less prone to failure. This might not be important for thick packages with small chips, but can have an appreciably adverse effect on the reliability of thin packages with large chips. In this connection we would like to point out that, from the Structural Analysis standpoint, the difference between "thin" and "thick" packages is due, first of all, to whether the membrane stresses contribute substantially, or not, to the total maximum stress in the molding compound.

Effective Young's moduli. Effective Young's moduli E_C and E_D in tension and bending can be always evaluated numerically. It is more convenient, however, to compute them on the basis of approximate formulas. In this section we derive such formulas assuming that the actual distribution of Young's modulus of the molding material in the through-thickness direction can be approximated by a parabola:

$$E(z_1) = E_0[2(e_+ + e_- - 2)\zeta^2 - (3e_+ + e_- - 4)\zeta + e_+], \tag{74}$$

where $\zeta = z_1/h$ is the dimensionless through-thickness coordinate, counted from the external ("hot") surface of the plate, E_0 is Young's modulus value in the midplane, and $e_+ = E_+/E_0$ and $e_- = E_-/E_0$ are the ratios of Young's moduli E_+ and E_- on the "hot" and the "cold" surfaces of the plate, respectively, to the midplane Young's modulus E_0.

With the expression (74), eqns (5) and (7) result in the following approximate formulae:

$$E_D = E_0 \frac{8(e_+ + e_- + e_+ e_- + 1) - (e_+^2 + e_-^2)}{5(e_+ + e_- + 4)}, \quad E_c = E_0 \frac{e_+ + e_- + 4}{6}, \tag{75}$$

which can be used in engineering calculations.

Total in-plane ("membrane") stress. The total transverse in-plane stress (i.e., the stress acting along the short side of the plate), calculated with consideration of the effect of the change in the coefficient of thermal expansion α, can be determined, in accordance with the formulae (11), as follows:

$$\sigma_x^0 = E\left[C(N_x + N_T) - \frac{\alpha \Delta T}{1-v}\right] = \frac{E}{E_c}\tilde{\sigma}_x^0 + \frac{E}{1-v}\left(\frac{1}{E_c h}\int_{-z_c}^{h-z_c} E\alpha\Delta T \, dz - \alpha\Delta T\right). \tag{76}$$

The thermally induced strain $\alpha\Delta T$ decreases, and the Young's modulus E of the molding compound increases, with the decrease in temperature. Therefore, in an approximate analysis, one can assume that the thermally induced stress $E\alpha\Delta T$ remains constant over the plate's thickness. With such a simplification, one can write the formula (75) as follows:

$$\sigma_x^0 = \frac{E}{E_c}\left(\tilde{\sigma}_x^0 + \frac{E-E_c}{1-\nu}\alpha\,\Delta T\right). \tag{77}$$

Clearly, for $E = E_c$, the total stress $\sigma_x^0 =$ becomes equal to the "mechanical" stress $\tilde{\sigma}_x^0$. Similarly to (76), the total longitudinal in-plane stress (i.e., the stress acting in the direction of the long side of the plate) can be calculated as

$$\sigma_y^0 = \frac{E}{E_c}\left(\tilde{\sigma}_y^0 + \frac{E-E_c}{1-\nu}\alpha\,\Delta T\right) = \frac{E}{E_c}\left(\nu\tilde{\sigma}_x^0 + \frac{E-E_c}{1-\nu}\alpha\,\Delta T\right). \tag{78}$$

Von-Mises stress

Von-Mises stress (see, e.g., Timoshenko and Woinowski-Krieger, 1959) is defined as

$$\sigma_M = \frac{1}{\sqrt{2}}\sqrt{(\sigma_1-\sigma_2)^2+(\sigma_2-\sigma_3)^2+(\sigma_3-\sigma_1)^2}. \tag{79}$$

Here, σ_1, σ_2, and σ_3 are the principal stresses. In the case of a plate (two-dimensional state of stress), the principal stress σ_3 is zero, and therefore

$$\sigma_M = \sqrt{\sigma_1^2+\sigma_2^2-\sigma_1\sigma_2}. \tag{80}$$

The principal stress σ_1 in the transverse direction (in the direction of the x axis) is due to the bending stress σ_b and the in-plane ("membrane") stress σ_x^0, and can be evaluated as

$$\sigma_1 = \sigma_b + \sigma_x^0.$$

As to the principal stress σ_2, acting in the y direction, it is due, in the case of an elongated plate, to the membrane stress σ_y^0 only, so that $\sigma_2 = \sigma_y^0$. Then the formula (79) yields:

$$\sigma_M = \sigma_b\left\{1+(2-\nu)\eta^2+(1-\nu+\nu^2)\eta+[1+(1+\nu)\eta]\eta\frac{\alpha\,\Delta T}{1-\nu}\frac{E-E_c}{\tilde{\sigma}_x^0}\right\}^{1/2}, \tag{81}$$

where the parameter η is expressed as

$$\eta = \frac{E}{E_c}\frac{\tilde{\sigma}_x^0}{\sigma_b}. \tag{82}$$

Simplified approach

Although the general analytical stress model, based on the constitutive eqns (1), accounts for any distribution of temperature in the molding component, in a simplified model one can consider the case when the temperature changes in the through-thickness direction only. It is believed that such a simplification is justified for many plastic package designs, especially for thin packages, in which the expected stresses are the highest. This situation is described by eqns (16). The solution to these equations is given in the Appendix.

In a simplified engineering approach one can use the following calculation procedure. The input data are: chip width, c, paddle width, a, underchip thickness, h, Young's modulus, E, and the coefficient of thermal expansion, α, of the molding compound as a function of temperature, Poisson's ratio of the molding compound, Young's moduli and coefficients of expansion of the chip and paddle materials (these are needed only if the stresses due to the thermal expansion mismatch of the constituent materials are considered), and the water vapor pressure, p. The calculations can be carried out in the following sequence:

1. For the given temperature gradient, calculate the distribution of Young's moduli in the through-thickness direction, and compute equivalent Young's moduli E_D (from the standpoint of bending) and E_C (from the standpoint of in-plane deformations) by the formulae (15) and (10).
2. For the given thickness-to-width ratio h/a and the computed p/E_D ratio of the lateral pressure p to the effective Young's modulus E_D in bending, determine the pressure factor χ_p from the formula (71).
3. For the given c/a ratio of the width c of the loaded area (chip's width) to the width a of the plate,and the calculated χ_p value, determine the value of the parameter u, characterizing the role of the in-plane ("membrane") stresses, on the basis of the plot in Fig. 6.
4. For the given c/a ratio and the computed u value, calculate the factors χ_f and χ_M, reflecting the effects of the c/a and u values on the maximum deflection and the maximum bending moment. These factors can be calculated on the basis of the formulas (49) and (55), or the plots in Figs 4 and 5, respectively.
5. Determine the maximum bending stress σ_b by the formula (53), the maximum mechanical in-plane stress $\tilde{\sigma}_x^0$ by the formula (72), and the parameter η, reflecting the effect of the ratio of these stresses, by the formula (81).
6. Compute the von-Mises stress by the formula (80).

NUMERICAL EXAMPLES

(1) Let the temperature gradient in the through-thickness direction for the delaminated portion of the molding compound be such that Young's modulus of the material is $E_4 = 0.10 \times 10^6$ psi $= 70.3$ kg/mm^2 on the "hot" (external) side of the package, $E_- = 0.15 \times 10^6$ psi $= 105.5$ kg/mm^2 on the "cold" (facing the die) side, and $E_0 = 0.20 \times 10^6$ psi $= 140.6$ kg/mm^2 in the midplane area. Then, the formulae (15) and (10) result in the following effective Young's moduli: $E_D = 0.1538 \times 10^6$ psi $= 108.1$ kg/mm^2, $E_C = 0.1750 \times 10^6$ psi $= 123.1$ kg/mm^2.

Let the pressure of the water vapor be $p = 360$ psi $= 0.253$ kg/mm^2 (this corresponds to the pressure of a saturated vapor at 220°C), the width of the delaminated portion be $a = 20$ mm, and its thickness be $h = 1$ mm. Assuming for Poisson's ratio $\nu = 0.4$, the formula (71) yields: $\bar{p} = \chi_p = 28.25$. Let the chip be $c = 10$ mm wide, and therefore $c/a = 0.5$. Then the plot in Fig. 6 yields: $u = 5.65$, and formula (70) results in the following deflection-to-thickness ratio: $f/h = 1.966$. Hence, the maximum deflection is almost twice as large as the plate's thickness (the thickness of the delaminated compound).

From the plot in Fig. 5, for $c/a = 0.5$ and $u = 5.65$, we obtain: $\chi_M = 0.26$. In the case, when there are no "membrane" stresses and the lateral load is distributed over the entire width of the delaminated compound, the bending stress σ_0, as predicted by formula (54), would be $\sigma_0 = 72{,}000$ psi $= 50.6$ kg/mm^2. Thus, the fact that the tensile force is not zero and the lateral load acts only in the midportion of the package, leads to a substantial, almost by a factor of four, reduction of the bending stress: $\sigma_b = \chi_M \sigma_0 = 0.26 \times 72{,}000 = 8720$ psi $= 6.13$ kg/mm^2.

The "mechanical" transverse in-plane stress (acting in the x direction) can be determined by the formula (69): $\tilde{\sigma}_x^0 = 4870$ psi $= 3.42$ kg/mm^2. From (81) we obtain: $\eta = 0.2230$. Let the coefficient of thermal expansion of the compound be $\alpha = 60 \times 10^{-6}$ 1/°C, and the change in temperature from the curing temperature to the reflow soldering temperature be $\Delta T = 80$°C. Then, formula (80) results in the following von-Mises stress: $\sigma_M = 22{,}016$ psi $= 15.5$ kgf/mm^2. This stress is high and can possibly result in the failure of the molding material.

(2) Let us determine now the maximum von-Mises stress for a square plate ($\gamma = 1$). In this case the formulae (A-17) and (A-18) of the Appendix yield: $\bar{f}_0 = 4.8444$ and $\alpha = 0.5965$. From (A-16) we find: $\mu = 27.9976$, $\eta_f = 0.3579$, and the formula (A-15) results in the following deflection-to-thickness ratio: $\bar{f} = f/h = 1.7340$. Comparing this result with the ratio $f/h = 1.9660$, obtained previously for an elongated plate, we conclude that the maximum deflection of the delaminated molding compound in a square package is smaller

than in an elongated one by a factor of about 1.13. Since the bending stress is proportional to the maximum deflection, this stress can be evaluated for a square plate (package) based on the decreased deflection and is $\sigma_b = 16{,}511$ psi $= 11.6$ kg/mm^2. The factors reflecting the effect of the finite aspect ratio on the in-plane stresses can be computed, using the formulae (A-11), and are as follows: $\psi_x^0(\gamma) = 0.8113$, $\psi_y^0(\gamma) = 1.6133$. The "mechanical" in-plane stresses can be then calculated as $\tilde{\sigma}_x^0 = 0.8113 \times 4870 = 3951$ psi $= 2.78$ kg/mm^2, and $\tilde{\sigma}_y^0 = 0.4 \times 4870 \times 1.6133 = 3143$ psi $= 2.21$ kg/mm^2. The total in-plane stresses are $\sigma_x^0 = 3279$ psi $= 2.31$ kg/mm^2, and $\sigma_y^0 = 1247$ psi $= 0.877$ kg/mm^2, and the principal stresses are $\sigma_1 = \sigma_b + \sigma_x^0 = 20{,}462$ psi $= 14.39$ kg/mm^2, and $\sigma_2 = \sigma_y^0 = 1247$ psi $= 0.877$ kg/mm^2. The predicted von-Mises stress is $\sigma_M = 19{,}868$ psi $= 14.0$ kgf/mm^2. This value is only a little lower than the calculated stress in an elongated plate of the same width.

(3) Let us assess now, whether an increase in the thickness of the molding compound can result in an appreciable decrease in the predicted von-Mises stress. Let the thickness of the delaminated portion of the compound be, say $h = 1.5$ mm, instead of $h = 1.0$ mm in the previous example. Then, from formula (71) one obtains: $\bar{p} = \chi_p = 5.580$. From the plot in Fig. 6 we find: $u = 2.65$, and formula (70) yields: $f/h = 0.9221$. The absolute deflection is $f = 1.383$ mm and is substantially lower than the deflection $f = 1.966$ mm in the case of a 1 mm thick compound. The bending stress, calculated in the absence of the "membrane" forces for a load distributed over the entire width of the plate, is $\sigma_0 = 32{,}000$ psi $= 22.5$ kg/mm^2. The factor χ_M, considering the effects of the finite c/a ratio and the tensile stress on the maximum bending moment, is $\chi_M = 0.20$, and the predicted stress is $\sigma_b = 6400$ psi $= 4.50$ kg/mm^2. This value is almost three times lower than in the case of a 1 mm thick compound. The "mechanical" in-plane stress, predicted by the formula (69), is $\tilde{\sigma}_x^0 = 2410$ psi $= 1.695$ kg/mm^2. From formula (81) we find: $\eta = 0.3228$, and the formula (80) results in the following von-Mises stress: $\sigma_M = 8023$ psi $= 5.64$ kgf/mm^2. Thus, an increase in the thickness of the molding compound by a factor of 1.5 led to a 2.74-fold reduction in the von-Mises stress.

CALCULATED DATA

The maximum von-Mises stresses calculated for several actual plastic package designs are shown in Table 1. The calculated data are in satisfactory agreement with the experimental observations. As evident from these data, the level of the calculated stress varies significantly depending on the particular package design.

Table 1. Numerical results

Package type	Die size, c (mm)	Paddle size, a (mm)	Thickness, h (mm)	Cracked (*)	Calculated Von-Mises stress, σ_M (kg/mm^2)
Vendor #1					
132 PQFP	8.910 × 8.700	10.160 × 10.160	1.702	no	4.465
164 PQFP	8.520 × 8.310	10.668 × 10.668	1.702	no	4.755
100 TQFP	6.850 × 6.950	8.001 × 8.001	0.660	yes	14.956
28 SOJ	3.549 × 4.679	7.620 × 4.826	1.041	no	4.478
44 PLCC	9.000 × 8.580	9.398 × 9.398	1.778	no	3.556
68 PLCC	6.700 × 6.760	8.890 × 8.890	1.930	no	2.474
84 PLCC	8.130 × 8.130	9.144 × 9.144	1.803	no	3.221
160 EIAJ	6.810 × 10.520	7.391 × 11.709	1.626	no	2.605
Vendor #2					
68 PLCC	4.200 × 4.200	6.800 × 6.800	1.513	no	0.301
Vendor #3					
32 PLCC	6.800 × 5.600	8.900 × 7.380	1.090	no	2.810
Vendor #4					
44 PLCC	8.100 × 6.500	9.000 × 9.000	1.579	no	1.617
Vendor #5					
80 PQFP	8.132 × 8.078	9.205 × 9.201	0.600	yes	16.477
Vendor #6					
240 PQFP	9.650 × 9.410	12.790 × 12.780	1.286	no	5.421

* 30°C/60% relative humidity/168 hrs (Ilyas and Poborets, 1993).

CONCLUSION

A calculation procedure has been developed for the evaluation of the failure criterion (von-Mises stress) for a moisture-sensitive plastic package during its surface mounting on a printed circuit board. A situation, when complete delamination between the molding compound and the chip (or the paddle) takes place, or is likely to occur during reflow soldering, is examined in detail, and a practical calculation procedure is developed for this case. This procedure can be effectively used to assess the role of different materials and geometrical characteristics on the von-Mises stress, and, hence, on the package propensity to structural failure. The developed stress model can also be applied for the preliminary separation of packages that need to be "baked" and "bagged" from those that do not. This model can be used also to judge whether qualification test conditions for reliable enough packages (say, thick packages with small chips) could be safely "derated" to an actual factory humidity profile. Finally, the calculated data obtained on the basis of the developed model can provide guidance for the selection of the most feasible molding compound for the given package design: highly reliable and expensive compounds might be necessary for thin packages with large chips, but may not be needed for thick packages with small chips.

Acknowledgement—The author acknowledges, with thanks, the contribution made by Dr John D. Weld, Bell Laboratories, who computerized the constitutive equations and carried out the calculations for several actual plastic package designs.

REFERENCES

Bhattachayya, B. K., Huffman, W. A., Jahshman, W. E. and Natarajan, B. (1988) Moisture absorption and mechanical performance of surface mountable plastic packages. In *IEEE 38th ECC Proc.*, Los Angeles, CA, pp. 49–58.

Cognett, C. (1988) Popcorn effect in reflow soldering of surface mounted assemblies in plastic housing. *Electronik* **37**, 116–120 (in German).

Conrad, T. R. and Shook, R. L. (1994) Impact of moisture/reflow induced delaminations on integrated circuit thermal performance. In *IEEE 44th ECTC Proc.*, Washington, DC, pp. 527–531.

EIA/JEDEC Standard (1995) Moisture-induced stress sensitivity for plastic surface mount devices. Test Method A112-A, Electronic Industries Association, Engineering Department, Arlington, VA.

Flood, C. A. and White, G. M. (1984) Desorption equilibrium moisture relationships for popcorn. *Transactions of the American Society of Agricultural Engineers* **27**, 561–565.

Fukuzawa, I., Ishiguro, S. and Nambu, S. (1985) Moisture resistance degradation of plastic LSI's by reflow soldering. In *23rd Int. Reliab. Physics Symp. Proc.*, Orlando, FL, pp. 192–197.

Ganssan, G. S. and Berg, H. (1993) Model and analyses for reflow cracking phenomenon in SMT plastic packages. In *IEEE 43rd ECTC Proc.*, pp. 653–660.

Ilyas, Q. S. M. and Poborets, B. (1993) Evaluation of moisture sensitivity of surface mount plastic packages. *Structural Analysis in Microelectronics and Fiber Optics*, EEP Vol. 7 (ed. E. Suhir), ASME, New Orleans, LA, pp. 145–156.

Ilyas, Q. S. M. and Potter, M. (1996) Experimental evaluation of moisture induced failures of surface mount plastic packages. In *IEEE 46th ECTC Proc.*, Orlando, FL, pp. 56–67.

IPC-SM-786 Standard (1992) Recommended procedures for handling of moisture sensitive plastic IC packages and IPC-Test Method 650-2.6.20. Plastic surface mount component cracking. IPC (Inst. for Interconnecting and Packaging Electronic Circuits), Lincolnwood, IL.

Klinger, D. J. (1991) Humidity acceleration factor for plastic packaged electronic devices. *Quality and Reliability Engineering International* **7**, 365–370.

Lea, C. and Tolbrook, D. (1989) Moisture induced failure in plastic surface mount packages. *Soldering and Surface-Mount Technology* **3**, 30–34.

Liu, S. (1993) Debonding and cracking of microlaminates due to mechanical and hydro-thermal loads for plastic packaging. In *Structural Analysis in Microelectronics and Fiber Optics*, EEP Vol. 7 (ed. E. Suhir), ASME, New Orleans, LA, pp. 1–11.

Miles, B. and Freyman, B. (1992) The elimination of the popcorn phenomenon in overmolded plastic pad array carriers. In *IEPS Proc.*, Vol. 1, pp. 605–614.

Pope, D. and Clifton, L. (1988) Package cracking in plastic surface mount components as a function of package moisture content and geometry. In *5th Ann. IEEE/IETM/CHMT Symp. Proc.*, pp. 89–92.

Shook, R. L. (1992) Moisture sensitivity characterization of plastic surface mount devices using scanning acoustic microscopy. In *30th Int. Rel. Phys. Symp. Proc.*, pp. 157–168.

Shoraka, F. (1986) Package and molding compound mechanics. In *6th Ann. Int. Electr. Pack. Conf. Proc.*, pp. 294–312.

Steiner, T. and Suhl, D. (1987) Investigation of large PLCC package cracking during surface mount exposure. *IEEE CHMT Transactions* **CHMT10**, 209–216.

Suhir, E. (1991) *Structural Analysis in Microelectronics and Fiber Optics*, Vol. 1, Van-Nostrand Reinhold.

Suhir, E. (1993) Predicted bow of plastic packages of integrated circuit devices. *J Reinforced Plastics and Composites* **12**, 951–972.

Suhir, E. (1995) Failure criterion for moisture-sensitive plastic packages. In *IEEE 45th ECTC*, Las Vegas, NV, pp. 266–284.

Suhir, E. and Ilyas, Q. S. M. (1996) "Thick" plastic packages with "small" chips vs "thin" packages with "large" chips: how different is thin propensity to moisture-induced failure? In *Structural Analysis in Microelectronics and Fiber Optics* (ed. E. Suhir), ASME, Atlanta, GA, pp. 101–125.

Suzuki, S. and Oota, K. (1992) Analysis of solder crack phenomena in LSI plastic packages. In *Joint ASME/JSME Conf. on Electronic Pack. Proc.*, Milpstar, CA, pp. 343–347.

Tencer, M. (1994) Moisture ingress into nonhermetic enclosures and packages. A quasi-steady state model for diffusion and attenuation of ambient humidity variations. In *IEEE 44th ECTC Proc.*, Washington, DC, pp. 196–209.

Thompson, P. (1994) Reliability development and qualification of a low-cost PQFT-based MCM. In *IEEE 44th ECTC Proc.*, Washington, DC, pp. 186–190.

Timoshenko, S. P. and Woinowski-Krieger, S. (1959) *Theory of Plates and Shells*, 2nd edn., McGraw-Hill, New York.

van Doorselaer, K. and de Zeeuw, K. (1990) Relation between delamination and temperature cycling induced failures in plastic packaged devices. *IEEE CHMT Transactions* **CHMT-13,** 879–882.

van Vroonhoven, J. C. W. (1993) Effects of adhesion and delamination on stress singularities in plastic-packaged integrated circuits. *ASME Journal of Electronic Packaging* **115,** 28–33.

Yamada, S. E. (1992) A bonded joint analysis for surface mount components. *ASME Journal of Electronic Packaging* **114,** 1–7.

APPENDIX A: CLAMPED PLATE OF FINITE ASPECT RATIO EXPERIENCING LARGE DEFLECTIONS

If the temperature in a rectangular plate changes in the through-thickness direction only, then, for an initially flat and stress free plate, eqns (16) can be used to evaluate the deflections $w(x, y)$ and the stress function $\phi(x, y)$.

The functions $w(x, y)$ and $\phi(x, y)$ can be sought in the form (Suhir, 1991):

$$w(x, y) = fw^*(x, y), \quad \phi(x, y) = f^2\phi^*(x, y), \tag{A1}$$

where f is the maximum deflection at the center of the plate, the coordinate function $w^*(x, y)$ is chosen in such a way that the boundary conditions for the deflection function at the plate's contour be fulfilled, and the function ϕ^* is to be determined. Substituting the relationships (A1) into the second equation in (16), we obtain the following equation for the function $\phi^*(x, y)$:

$$\begin{aligned}\nabla^4\phi^*(x, y) &= -\frac{E_C}{2}L[w^*(x, y), w^*(x, y)]\\ &= E_C\left[\left(\frac{\partial^2 w^*}{\partial x\,\partial y}\right)^2 - \frac{\partial^2 w^*}{\partial x^2}\frac{\partial^2 w^*}{\partial y^2}\right],\end{aligned} \tag{A2}$$

where the equivalent modulus E_C is expressed by formula (10).

In an approximate analysis one can assume for a plate clamped at the support contour,

$$w^*(x, y) = \cos^2\frac{\pi x}{a}\cos^2\frac{\pi y}{b}. \tag{A3}$$

Then the equation (A2) yields:

$$\begin{aligned}\nabla^4\phi^*(x, y) = -\frac{\pi^4 E_0}{2a^2b^2}\bigg(&\cos\frac{2\pi x}{a} + \cos\frac{2\pi y}{b} + \cos\frac{4\pi x}{a} + \cos\frac{4\pi y}{b} + 2\cos\frac{2\pi x}{a}\cos\frac{2\pi y}{b}\\ &+ \cos\frac{2\pi x}{a}\cos\frac{4\pi y}{b} + \cos\frac{4\pi x}{a}\cos\frac{2\pi y}{b}\bigg).\end{aligned} \tag{A4}$$

This equation has the following solution:

$$\begin{aligned}\phi^*(x, y) = Ax^2 + By^2 &+ D_0\cos\frac{2\pi x}{a} + D_1\cos\frac{2\pi y}{b} + D_2\cos\frac{4\pi x}{a} + D_3\cos\frac{4\pi y}{b} + D_4\cos\frac{2\pi x}{a}\cos\frac{2\pi y}{b}\\ &+ D_5\cos\frac{2\pi x}{a}\cos\frac{4\pi y}{b} + D_6\cos\frac{4\pi x}{a}\cos\frac{2\pi y}{b}.\end{aligned} \tag{A5}$$

Substituting the expression (A5) into eqn (A4) we obtain the formulae for the constants $D_0 \to D_6$. Introducing (A5) into the conditions (9) of the nondeformability of the contour, we determine the constants A and B. Then, the formula (A5) results in the following expression for the function ϕ^*.

$$\phi^*(x,y) = \frac{E_0}{32}\left\{\frac{3\pi^2}{2(1-\nu^2)}\left[\left(\frac{\nu}{a^2}+\frac{1}{b^2}\right)x^2+\left(\frac{1}{a^2}+\frac{\nu}{b^2}\right)y^2\right]-\frac{a^2}{b^2}\cos\frac{\pi x}{a}-\frac{b^2}{a^2}\cos\frac{\pi y}{b}\right.$$
$$-\left(\frac{a}{4b}\right)^2\cos\frac{4\pi x}{a}-\left(\frac{b}{4a}\right)^2\cos\frac{4\pi y}{b}-\frac{2a^2b^2}{(a^2+b^2)^2}\cos\frac{2\pi x}{a}\cos\frac{2\pi y}{b}$$
$$\left.-\frac{a^2b^2}{(4a^2+b^2)^2}\cos\frac{2\pi x}{a}\cos\frac{4\pi y}{b}-\frac{a^2b^2}{(a^2+4b^2)^2}\cos\frac{4\pi x}{a}\cos\frac{2\pi y}{b}\right\}. \quad \text{(A6)}$$

The in-plane stresses can be then evaluated as follows:

$$\left.\begin{aligned}
\sigma_x^0 &= \frac{\partial^2\phi}{\partial y^2} = f^2\frac{\partial^2\phi^*}{\partial y^2} = \frac{\pi^2E_0f^2}{32}\left[\frac{3}{1-\nu^2}\left(\frac{1}{a^2}+\frac{\nu}{b^2}\right)+\frac{1}{a^2}\cos\frac{\pi y}{b}+\frac{1}{a^2}\cos\frac{4\pi y}{b}\right.\\
&\quad\left.+\frac{8a^2}{(a^2+b^2)^2}\cos\frac{2\pi x}{a}\cos\frac{2\pi y}{b}+\frac{16a^2}{(4a^2+b^2)^2}\cos\frac{2\pi x}{a}\cos\frac{4\pi y}{b}+\frac{4a^2}{(a^2+4b^2)^2}\cos\frac{4\pi x}{a}\cos\frac{2\pi y}{b}\right],\\
\sigma_y^0 &= \frac{\partial^2\phi}{\partial x^2} = f^2\frac{\partial^2\phi^*}{\partial x^2} = \frac{\pi^2E_0f^2}{32}\left[\frac{3}{1-\nu^2}\left(\frac{\nu}{a^2}+\frac{1}{b^2}\right)+\frac{1}{b^2}\cos\frac{\pi x}{a}+\frac{1}{b^2}\cos\frac{4\pi x}{a}\right.\\
&\quad\left.+\frac{8b^2}{(a^2+b^2)^2}\cos\frac{2\pi x}{a}\cos\frac{2\pi y}{b}+\frac{16b^2}{(a^2+4b^2)^2}\cos\frac{4\pi x}{a}\cos\frac{2\pi y}{b}+\frac{4b^2}{(4a^2+b^2)^2}\cos\frac{2\pi x}{a}\cos\frac{4\pi y}{b}\right],\\
\tau_{xy}^0 &= -\frac{\partial^2\phi}{\partial x\,\partial y} = -f^2\frac{\partial^2\phi^*}{\partial x\,\partial y} = \frac{\pi^2E_0abf^2}{4}\left[\frac{1}{(a^2+b^2)^2}\sin\frac{2\pi x}{a}\sin\frac{2\pi y}{b}\right.\\
&\quad\left.+\frac{1}{(4a^2+b^2)^2}\sin\frac{2\pi x}{a}\sin\frac{4\pi y}{b}+\frac{1}{(a^2+4b^2)^2}\sin\frac{4\pi x}{a}\sin\frac{2\pi y}{b}\right].
\end{aligned}\right\} \quad \text{(A7)}$$

At the point $x = a/2$, $y = 0$, the formulae (A7) yield:

$$\sigma_x^0 = [\sigma_x^0]_\infty\psi_x^0(\gamma), \quad \sigma_y^0 = [\sigma_y^0]_\infty\psi_y^0(\gamma), \quad \text{(A8)}$$

where

$$\left.\begin{aligned}
[\sigma_x^0]_\infty &= \frac{5-2\nu^2}{1-\nu^2}\frac{\pi^2E_0f^2}{32a^2}\\
[\sigma_y^0]_\infty &= \frac{3\nu}{1-\nu^2}\frac{\pi^2E_0f^2}{32a^2}
\end{aligned}\right\} \quad \text{(A9)}$$

are the in-plane stresses, calculated for the case of an elongated plate ($b \to \infty, \gamma = 0$), and the factors

$$\left.\begin{aligned}
\psi_x^0(\gamma) &= 1+\frac{3\nu}{5-2\nu^2}\gamma^2-\frac{4(1-\nu^2)}{5-2\nu^2}\gamma^4\left[\frac{2}{(1+\gamma^2)^2}+\frac{4}{(1+4\gamma^2)^2}-\frac{1}{(4+\gamma^2)^2}\right]\\
\psi_y^0(\gamma) &= 1+\frac{2+\nu^2}{3\nu}\gamma^2-\frac{4(1-\nu^2)}{3\nu}\gamma^4\left[\frac{2}{(1+\gamma^2)^2}+\frac{1}{(1+4\gamma^2)^2}-\frac{4}{(4+\gamma^2)^2}\right]
\end{aligned}\right\} \quad \text{(A10)}$$

reflect the effect of the finite aspect ratio $\gamma = a/b$. The shear stress at the point $x = a/2$, $y = 0$ is zero.

For an elongated plate ($\gamma = 0$) the formulae (A10) yield: $\psi_x^0(1) = \psi_y^0(0) = 1$. For a square plate ($\gamma = 1$) these formulae result in the expressions:

$$\psi_x^0 = \frac{(1+\nu)(63+12\nu)}{25(5-2\nu^2)}, \quad \psi_y^0 = 1+\frac{4(3+10\nu^2)}{75\nu}. \quad \text{(A11)}$$

If, for instance, $\nu = 0.4$, then $\psi_x^0 = 0.8113$ and $\psi_y^0 = 1.6133$. Hence, the finite aspect ratio of the plate results in lower in-plane stresses in the x direction and in higher stresses in the y direction.

The first equation in (16) can be solved, using the Galerkin method (see, for instance, Timoshenko and Woinowski-Krieger, 1959). In accordance with the procedure of this method, we substitute the formulae (A1), with consideration of (A2), into the first equation in (16), multiply the obtained expression by the coordinate function $w^*(x, y)$, and integrate the result over the plate's surface A. This leads to the following equation for the dimensionless deflection $\bar{f} = f/h$:

$$\bar{f}+\alpha\bar{f}^3=\bar{f}_0, \tag{A12}$$

where

$$\bar{f}_0=\frac{1}{Dh}\frac{\int_A p(x,y)w^*(x,y)\,\mathrm{d}A}{\int_A w^*(x,y)\nabla^4 w^*(x,y)\,\mathrm{d}A} \tag{A13}$$

is the dimensionless linear deflection ($\alpha = 0$), and

$$\alpha=-\frac{h^3}{D}\frac{\int_A w^*(x,y)L[w^*(x,y),w^*(x,y)]\,\mathrm{d}A}{\int_A w^*(x,y)\nabla^4 w^*(x,y)\,\mathrm{d}A} \tag{A14}$$

is the parameter of nonlinearity. The solution to eqn (A12) can be written as follows:

$$\bar{f}=\eta_f\bar{f}_0, \tag{A15}$$

where the factor

$$\eta_f=\frac{1}{\sqrt[3]{\mu}}\left(\sqrt[3]{1+\sqrt{1+\frac{8}{27\mu}}}+\sqrt[3]{1-\sqrt{1+\frac{8}{27\mu}}}\right),\quad \mu=2\alpha\bar{f}_0^2 \tag{A16}$$

considers the effect of the nonlinearity ("membrane" stresses).

Introducing (A3) into formulae (A13) and (A14), we obtain:

$$\bar{f}_0=\frac{pa^4}{\pi^4 D(3+2\gamma^2+3\gamma^4)h}=\frac{12}{\pi^4}\frac{p}{E_D}\frac{1-\nu^2}{3+2\gamma^2+3\gamma^4}\left(\frac{a}{h}\right)^4, \tag{A17}$$

$$\alpha=\frac{3(1-\nu^2)}{8(3+2\gamma^2+3\gamma^3)}\left[\frac{9}{4}\frac{1+2\nu\gamma^2+\gamma^4}{1-\nu^2}+\frac{17}{8}(1+\gamma^4)+\frac{12\gamma^4}{(1+\gamma^2)^2}+\frac{5\gamma^4}{(1+4\gamma^2)^2}+\frac{5\gamma^4}{(4+\gamma^2)^2}\right]. \tag{A18}$$

Using formulae (12) for the bending moments acting in the plate's cross-sections, putting $M_T = 0$, and considering the first formula in (A1), we have:

$$\left.\begin{aligned}M_x&=-Df\left(\frac{\partial^2 w^*}{\partial x^2}+\nu\frac{\partial^2 w^*}{\partial y^2}\right)\\ M_y&=-Df\left(\frac{\partial^2 w^*}{\partial y^2}+\nu\frac{\partial^2 w^*}{\partial x^2}\right)\\ M_{xy}&=-D(1-\nu)f\frac{\partial^2 w^*}{\partial x\,\partial y}\end{aligned}\right\}. \tag{A19}$$

Using eqn (A3), we obtain:

$$\left.\begin{aligned}M_x&=2\pi^2 Df\left(\frac{1}{a^2}\cos\frac{2\pi x}{a}\cos\frac{2\pi y}{b}+\frac{\nu}{b^2}\cos\frac{2\pi y}{b}\cos\frac{2\pi x}{a}\right)\\ M_y&=2\pi^2 Df\left(\frac{1}{b^2}\cos\frac{2\pi y}{b}\cos\frac{2\pi x}{a}+\frac{\nu}{a^2}\cos\frac{2\pi x}{a}\cos\frac{2\pi y}{b}\right)\\ M_{xy}&=-D(1-\nu)f\frac{\pi^2}{ab}\sin\frac{2\pi x}{a}\sin\frac{2\pi y}{b}\end{aligned}\right\}.$$

At the point $x = a/2$, $y = 0$, these formulae yield:

$$M_x = -\frac{2\pi^2}{a^2}Df, \quad M_y = -\frac{2\pi^2}{a^2}\nu Df, \quad M_{xy} = 0.$$

The bending stresses caused by these moments can be calculated as follows:

$$\sigma_x = -\frac{6M_x}{h^2} = \frac{12\pi^2 Df}{a^2h^2}, \quad \sigma_y = -\frac{6M_y}{h^2} = \frac{12\pi^2 \nu Df}{a^2h^2}. \tag{A20}$$

In the case of an elongated plate ($b \to \infty, \gamma = 0$), formula (A17) yields:

$$\bar{f}_\infty = \bar{f}_0 = \frac{pa^4}{3\pi^4 Dh}.$$

Using this formula and formula (A15), one can calculate the factor $\eta^* = \bar{f}/f_\infty = \eta_f(\bar{f}_0/f_\infty)$, which considers the effect of the finite aspect ratio of the plate on its maximum deflection.